

Identifying Dominant Factor of Imbalance Component and EM Radiation from Differential-Paired Lines with Serpentine Equi-Length Routing

Yoshiki KAYANO

Department of Electrical and Electronic Engineering,
Akita University
1-1 Tegata-gakuen-machi, Akita-shi, 010-8502, Japan
Email: kayano@gipc.akita-u.ac.jp

Hiroshi INOUE

Akita Study Center,
The Open University of Japan
1-1 Tegata-gakuen-machi, Akita-shi, 010-8502, Japan
Email: inoueh@gipc.akita-u.ac.jp

Abstract—For actual differential-signaling system, the ideal balance or symmetrical topology cannot be established, and hence, an imbalance component is excited. To provide the basic considerations for establishment of predicting the EM radiation from practical differential-paired lines, this paper attempts to identify the dominant factor of imbalance component and EM radiation from asymmetrical differential-paired line with equi-length routing.

Keywords—*equi-length routing, bend, imbalance, EMI*

I. INTRODUCTION

Multi-channel Differential-signalling techniques are widely used in high-speed multi-channel transmission line. In actual differential-paired lines, there are the skew and distortion of the traveling-waveform generated by the non-ideal symmetrical topology due to a bend (turnoff point) discontinuity and topology such as a serpentine. Imbalance components (common-mode: CM) between voltages waveforms traveling the differential paired lines due to a bend region deteriorate signal integrity (SI) and intensify EMI. Many papers have published to contribute the suppression and compensation of imbalance component due to the bend region [1]–[3]. But many of these conventional studies had been mainly focused on either SI or EMI issue. Therefore general study for predicting and suppressing EMI as well as establishment of signal integrity over a broad band are required.

The previous studies from view point of both SI and EMI [4]–[6] have demonstrated that although the conversion parameter from DM (balance component) to CM (imbalance component) $|S_{cd21}|$ can be suppressed by the equi-length routing, it is not considered for the suppression of the radiated emission. More importantly, the $|S_{cd21}|$ is not a single evaluator for predicting the EM radiation. It is helpful to be able to anticipate at the design stage the dominant radiation factor. Also by knowing them, EMI design guidelines can be developed. Against this background, the authors have proposed the physics-based model for prediction and identification of the dominant radiation factor [5]. The case of simple asymmetrical differential-paired lines had been reported successfully. However, due to the difficulty of applying the theory to complex geometries, the correlation between generation of imbalance component and EM radiation from practical multiple bend routing such as a serpentine has not yet been cleared com-

pletely, which allows to study possible means for suppressing EMI for practical applications.

The main goal of this study is to clarify the characteristics and dominant radiation factor of such PCBs and to acquire basic insights for designing way for both SI and EMI performances of differential-paired lines. To provide the basic considerations for EM radiation from practical asymmetrical differential-paired lines structure with bend routing, we newly attempt to identify and quantify the dominant factor of imbalance component and EMI from strong and weak coupled differential-paired lines with serpentine equi-length routing. The PCB geometries used in the study are described in Section 2. In Section 3, the mixed-mode scattering parameters are discussed, from view point of SI performance. In Section 4, the far-electric field radiated from the PCB are discussed, from view point of EMI.

II. PCB GEOMETRY UNDER STUDY

The differential-paired lines with different layouts were prepared for the discussion as typical different and equi-length routing. The geometries and cross-sectional view of the PCBs under study for appropriate simple model for studying and getting physical-insights are illustrated in Figs. 1. a) is a ideally balanced (symmetrical) layout, called “Balanced”. b) is a typical asymmetrical equi-length routing layout due to U-shape bend routing region, called “One U-shape”. c) is symmetrical topology with two U-shape bend regions as odd-function to x -axis, called “Two U-shape-Sym”. d) is asymmetrical topology with two U-shape bend regions as even-function to y -axis, called “Two U-shape-Asym”. e) is U-shape bend region only for comparison. The geometrical length of each lines in model (a) to (e) is the same.

The PCB has cross sectional three layers, with the upper layer for the signal trace, middle layer for the dielectric substrate and the lower layer for the reference (ground) plane. The size of the microstrip line structure used for the test model is $l=142$ mm (length), $w=100$ mm (width), and $h=1.53$ mm (thickness) for the dielectric substrate with a relative permittivity of $\epsilon_r=4.5$. Two traces with width $w_t=1.9$ mm, and spacing s are located on the surface of the dielectric substrate. As the focuses in this paper are on the imbalance component generated by asymmetrical topologies, the relatively wide separation $s=1.0$ mm is selected so that an imbalanced component due

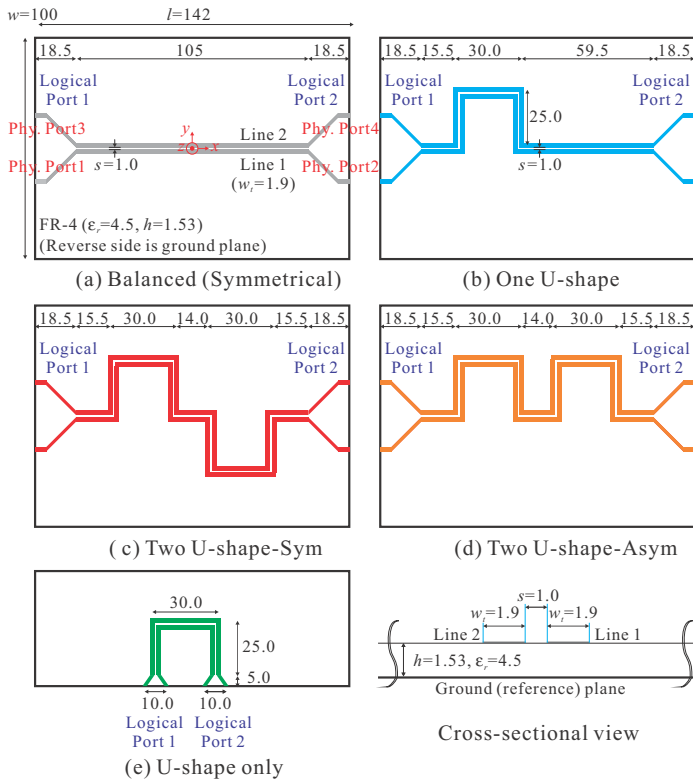


Fig. 1. Geometries of the PCBs under study (in mm).

to the asymmetrical structure is the dominant fact of the EM radiation compared with that due to the waveform distortion of the output of the LVDS driver. A symmetrical differential-paired lines has the differential mode impedance $Z_{DM}=100 \Omega$.

III. IMBALANCE COMPONENT ON DIFFERENTIAL-PAIRED LINES STRUCTURE

A. Evaluation of Mixed-Mode S parameter

The frequency responses of mixed-mode scattering parameters are shown in Figs. 2 and 3. The solid and broken lines show the measured results from the network analyzer with 4 ports, and the calculated results by FDTD (Finite-Difference Time-Domain) method, respectively. Figure 2 shows the measured frequency responses of $|S_{dd21}|$, which is defined as the transmission coefficient of the differential-mode. There is no remarkable difference in all cases up to 5 GHz. The deterioration (loss) of $|S_{dd21}|$ above 5 GHz is due to the dielectric loss of FR-4 substrate. Hence, the loss increases larger as the trace length becomes longer. Nevertheless, there is no resonance and anti-resonance due to the bend-routing.

Figure 3 shows the frequency responses of $|S_{cd21}|$, which is defined as the conversion from differential-mode (balance component) to common-mode (imbalance component). (a) and (b) are measured and calculated results, respectively. The measured and calculated results are in good agreement except the higher frequency above the 10 GHz.

The dominant factor of generation of imbalance component of the “U-shape only” case is the response of the geometrical length between Line 1 and 2 due to the bend routing. Therefore

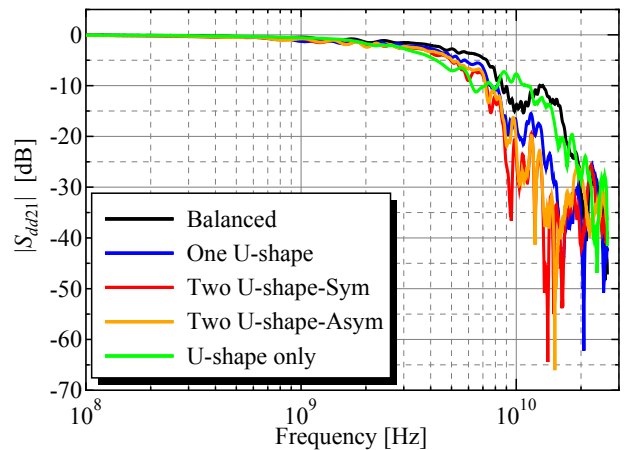
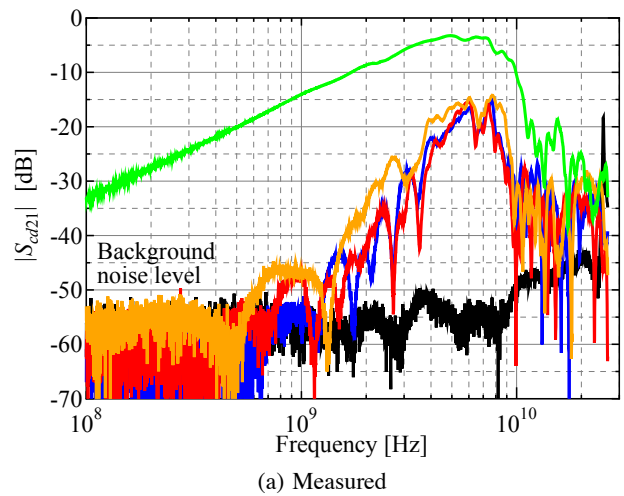
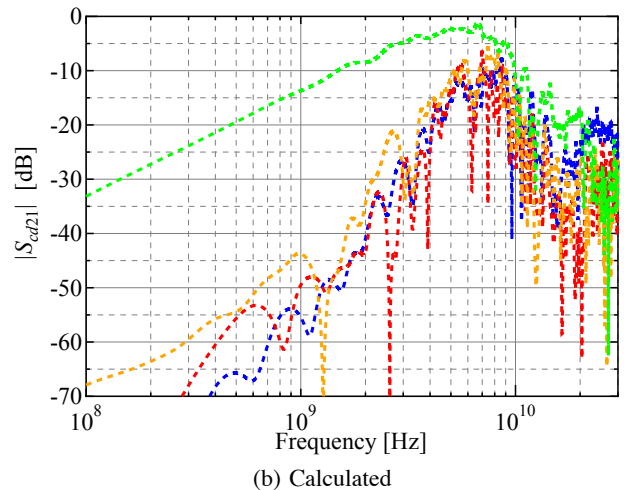


Fig. 2. Frequency responses of $|S_{dd21}|$.



(a) Measured



(b) Calculated

Fig. 3. Frequency responses of $|S_{cd21}|$. The lines in Fig. 3 correspond to the legends shown in Fig. 2.

the “U-shape only” case has slope of 6 dB/octave at lower frequency and is the worst case. By comparing the results for the “U-shape only” and other case, the equi-length routing can suppress the $|S_{cd21}|$ as it has been demonstrated in former studies [4]. Although the geometrical total length of each

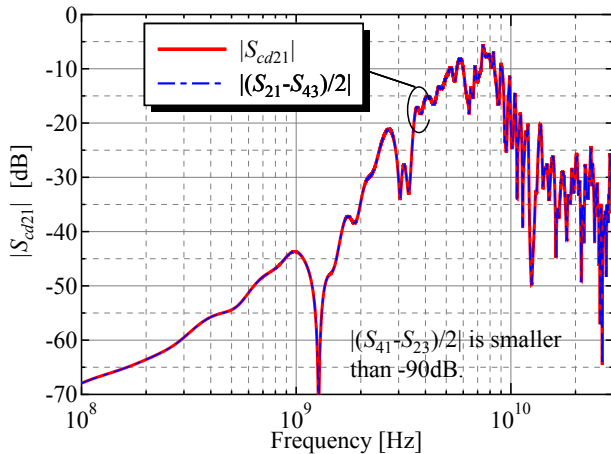


Fig. 4. Identification of dominant imbalance component in the “Two U-shape-Asym” case.

line is the same, $|S_{cd21}|$ exists and depends on the layout, that means an incomplete compensation. The $|S_{cd21}|$ in the “Two U-shape-Asym” case is larger than that in the “Two U-shape-Sym” case. The slopes of the frequency responses of $|S_{cd21}|$ in the “One U-shape” and “Two U-shape-Sym” at lower frequencies are tighter than that in the “Two U-shape-Asym” case

B. Dominant Factor of Imbalance Component

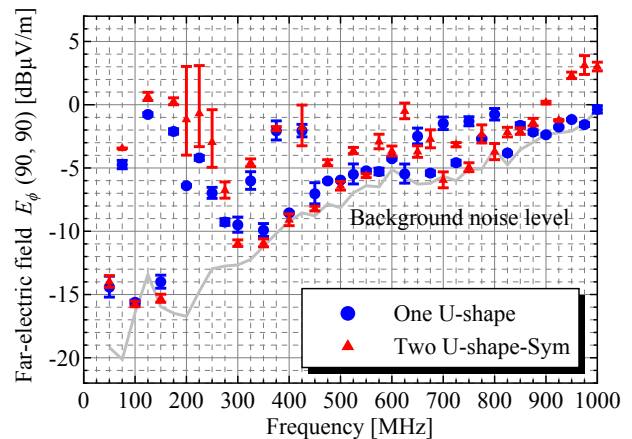
In order to identify the dominant generation factor of the imbalance component, the single-end s -parameters are calculated. The single-end s -parameter is related to Mixed-mode s -parameter:

$$S_{cd21} = \frac{S_{21} - S_{43} + S_{41} - S_{23}}{2}. \quad (1)$$

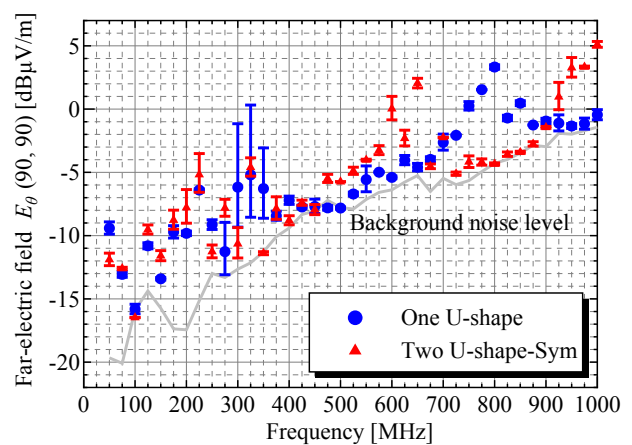
The calculated frequency responses of single-end s -parameter in the “Two U-shape-Asym” case are shown in Fig. 4. Figure 4 clearly demonstrates that the dominant factor of generation of imbalance component of the model under study is difference of the transmission path due to the asymmetrical geometry. Although the geometrical length of each line is the same, $|S_{cd21}|$ exists that means an incomplete compensation. Consequently, since frequency responses of phase-difference between two traces are 6 dB/octave (20 dB/decade), the outline of frequency response of imbalance component $|S_{cd21}|$ follows 6 dB/octave.

IV. RADIATED EMISSION

Experiments are performed to discuss the correlation between imbalance component and EM radiation from the PCB. The far-electric field radiated from the PCB was measured in an anechoic chamber with a Bi-Log antenna (30–1000 MHz). In the coordinate system, ϕ is the counterclockwise angle in the x - y plane measured from the positive x axis, and θ is the angle from the positive z axis. The differential paired lines are driven by an LVDS driver (NS DS90LV047A), and a crystal oscillator with 3.3 V amplitude and 25.0 MHz oscillation frequency. The crystal oscillator, LVDS driver, and battery are fixed on the ground side, and are covered with a shield box (thin-sheet copper). The differential paired line is terminated with 100 Ω



(a) Horizontal component



(b) Vertical component

Fig. 5. Measured frequency responses of the far-electric field [6].

SMT resistor. The PCB was placed on a wooden table. The distance between the PCB and the antenna was 3 m. The RBW and VBW of the spectrum analyzer are 1 kHz and 100 Hz, respectively. Horizontal component E_ϕ at $(\phi, \theta)=(90^\circ, 90^\circ)$ and vertical component E_θ at $(\phi, \theta)=(90^\circ, 90^\circ)$ are discussed.

The measured far-electric fields are shown in Fig. 5. (a) and (b) are horizontal component and vertical component, respectively. The horizontal component in the “Two U-shape-Sym” case is relatively larger than that in the “One U-shape” case. This fact does not correspond to the feature of imbalance component evaluated from the $|S_{cd21}|$. More importantly, the result indicates that only the measurement of S_{cd21} is insufficient for predicting the EM radiation.

The FDTD method is used for the calculation of the far-electric fields. The FDTD model provides results for the “ideal balanced differential-signaling excitation”, which can focus on the effects of non-ideal asymmetrical structures and the discontinuity of DM impedance of differential paired lines. Figure 6 shows the frequency response of the far-electric field, obtained by FDTD modeling. To discuss the frequency response of the far-electric field from the point of view of radiation efficiency, the result is normalized to the case where the frequency response of the input voltage to the trace is a

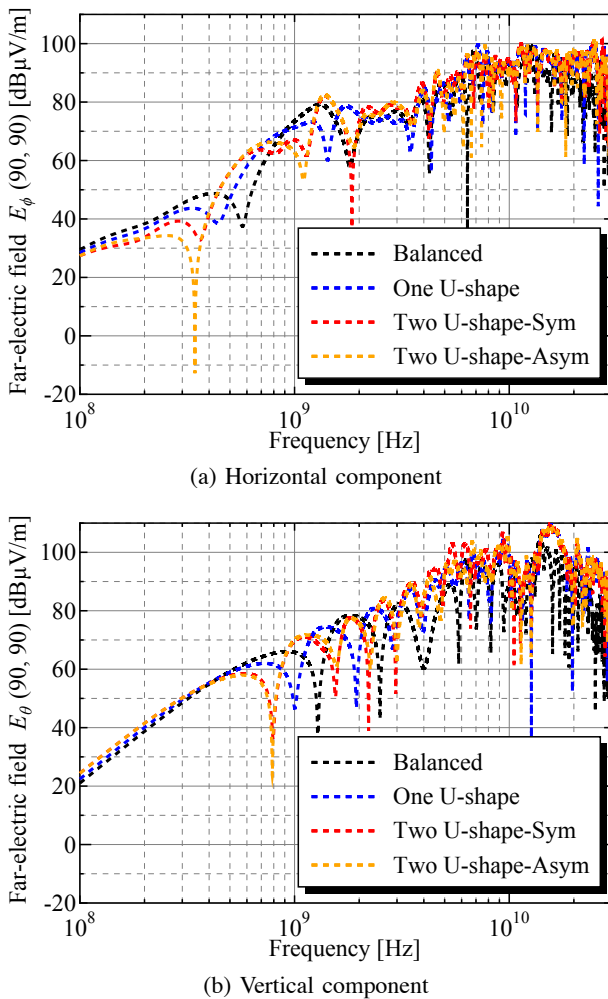


Fig. 6. Calculated frequency responses of the far-electric field in the case of “ideal balanced differential-signaling excitation”.

constant 1 V. As the frequency becomes higher, EM radiation increases. It is difficult to identify the resonant and anti-resonant characteristics by using the simple dipole and/or loop type antennas. But the physical-meanings of anti-resonant should be cleared for mitigating the EMI.

So far, three factors could be possible reasons why equi-length does not suppress EMI [4]. 1) There is a region of even-mode current propagation due to the asymmetric layout. The even-mode causes significant CM current and radiation as a CM dipole. 2) The spacing between the differential-paired lines at bend region becomes wider. Hence, the CM impedance decreases while the DM impedance increases. Additionally, the cancellation treatment for EM radiation at the observation point deteriorates dramatically. 3) The differential-paired lines are routed close to the edge of the PCB in the model layout. So, the CM current due to the finite impedance of the ground plane increases. Although the results do not allow us to distinguish the particular radiation component from each factor mentioned above, these consequences indicate that the “Two U-shape-Sym” case does not work as an effective treatment for suppressing EMI. The dominant factor of total far-electric field in the “Two U-shape-Sym” case may be considered radiated

component of factor 3. As the results, even if symmetrical equi-length routing is suitable for the improvement of SI issues, it cannot be expected to suppress the radiated emission. The factor 2 in the bend region may become more significant at higher frequencies.

The expected design guideline for differential-paired lines routing is to place to equi-routing near the phase-difference region and necessary “keep-out” area on the PCB edge whenever possible. Predicting the dominant component at a certain frequency band is a very important subject for mitigating EMI problems in high-speed electronic designs. The identifying the dominant radiation factor using the physics-based model and the simple dipole and/or loop type antennas should be further studies.

V. CONCLUSIONS

To provide basic considerations for the realization of methods for predicting and suppressing the EM radiation from asymmetrical differential-paired lines, the imbalance component and EMI from differential-paired lines with serpentine equi-length routing were studied experimentally and with modeling. Although serpentine equi-length routing is suitable for improvement of SI issues compared with typical layout, it is not effective in suppressing the EMI. The reason is due to the differential-paired lines routed close to the edge of the PCB. This is significant problem of design of a meander delay line for high-speed clock distribution to establish both SI and EMI performance. This study has successfully reported the basic characteristics of imbalance component of differential-paired lines with equi-length routing and demonstrates the dominant factor of imbalance component. The future subject is to establish a method for mitigating SI and EMI in high-speed electronic designs, by the acquired knowledge.

ACKNOWLEDGMENT

The authors sincerely thank to Mr. Yasunori Tsuda, Mr. Masashi Ohkoshi and Akita Industrial Technology Center, for their support of measurements,

REFERENCES

- [1] T.L. Wu, Y.H. Lin, T.K. Wang, C.C. Wang and S.T. Chen, “Electromagnetic Bandgap Power/Ground Planes for Wideband Suppression of Ground Bounce Noise and Radiated Emission in High-Speed Circuits”, *IEEE Trans. Microw. Theory Techn.*, vol.53, no.9, pp.2935–2942, Sep. 2005.
- [2] G.H. Shiue, J.H. Shiu, Y.C. Tsai and C.M. Hsu, “Analysis of Common-Mode Noise for Weakly Coupled Differential Serpentine Delay Microstrip Line in High-Speed Digital Circuits”, *IEEE Trans. Electromagn. Compat.*, vol.54, no.3, pp.655–666, Jun. 2012.
- [3] C.H. Chang, R.Y. Fang and C.L. Wang, “Bended Differential Transmission Line Using Compensation Inductance for Common-Mode Noise Suppression”, *IEEE Trans. Compon. Packag. Manuf. Technol.*, vol.2, no.9, pp.1518–1525, Sep. 2012.
- [4] Y. Kayano, K. Mimura and H. Inoue, “Evaluation of Imbalance Component and EM Radiation Generated by an Asymmetrical Differential-Paired Lines Structure”, *Trans. JIEP*, vol.4, no.1, pp.6–16, Dec. 2011.
- [5] Y. Kayano, Y. Tsuda and H. Inoue, “Identifying EM Radiation from Asymmetrical Differential-Paired Lines with Equi-Distance Routing”, in *Proc. IEEE Int. Symp. Electromagn. Compat.*, pp.311–316, Pittsburgh, PA, USA, Aug. 2012.
- [6] Y. Kayano and H. Inoue, “Imbalance Component and EM Radiation from Differential-Paired Lines with Serpentine Equi-Distance Routing”, in *Proc. IEEE Int. Symp. Electromagn. Compat.*, pp.359–364, Denver, CO, USA, Aug. 2013.